

24th COBEM - 2017



24th ABCM International Congress of Mechanical Engineering
December 3-8, 2017, Curitiba, PR, Brazil

COBEM-2017-2008

UNCERTAINTIES ON ADHESIVE LAYER FOR A CANTILEVER BEAM: PASSIVE CONTROL

Guilherme Silva Prado

Bryan Willys Goncalves

Heinsten Frederich Leal dos Santos

Universidade Federal de Mato Grosso

prado.gui@hotmail.com

Abstract. *Piezoelectric materials have been extensively studied in recent years for the development of electromechanical harvesting devices; however, much of the research that is available in open literature focuses on increasing mechanical and electrical performance, increasing efficiency, consequently harvesting. The conversion of mechanical energy to electric energy is provided by the electromechanical coupling between flexible structure and piezoceramic element. There are basically two types of strategies adopted when integrating piezoelectric sensors and actuators into flexible structures: bonding to the host structure surfaces or incorporation into a laminated structure of thin patches or layers of piezoelectric ceramics. In both cases, the interface between the host structure and the piezoelectric device plays a decisive role in terms of mechanical stress and voltage transfer mechanisms. This work presents a study on the influence of parametric uncertainties on the thickness properties and Young's modulus of adhesive bond strength, based on the expected statistical properties of variables, such as expected nominal value, dispersion and positivity.*

Keywords: *Piezoelectric materials, uncertainties, adhesive, energy harvesting*

1. INTRODUCTION

In several fields of engineering, analyzes are carried out in search of a project that presents high performance and, at the same time, reducing mass. Thus, the use of piezoelectric for the energy harvesting (through the direct effect), and vibration attenuation has a wide application as sensors and actuators, still highlighting the high energy efficient conversion between displacement and electric charge. That is why surface-mounted piezoelectric sensors and actuators are also known as extension or extension-bending sensors and actuators and were widely used an active (Sunar and Rao, 1999), passive (Reza Moheimani, 2003) and hybrid active-passive (Tang, Liu and Wang, 2000; Trindade and Benjeddou, 2002; Santos and Trindade, 2011) control applications.

The performance of piezoelectric patches for these types of applications are very much dependent on the adequate tuning between resonant, circuit and operation frequencies and on the effective electromechanical coupling between patches and host structure. Therefore, variabilities and/or uncertainties on material properties, boundary conditions and bonding effectiveness may have a major effect on reducing the expected or predicted performance of such devices (Santos and Trindade, 2012; Godoy and Trindade, 2012).

Still, most of the bonds made between piezoelectric inserts utilize two-part epoxy adhesives (resin and reinforcement), which must be cured at the ideal temperature and pressure to achieve the desired stiffness configuration, so that the curing and mixing process is very likely to be subject to uncertainties (Santos and Trindade, 2016).

Hence, the objective of the work is to present an analysis of the effect of uncertainties of bounding layer stiffness on the performance of piezoelectric sensors and actuators with application to passive shunted damping and energy harvesting. For that, the bounding layer Young Modulus is represented by a stochastic parameter and Monte Carlo simulations are performed to evaluate mean and confidence intervals of the damping and energy harvesting performance.

2. FINITE ELEMENT MODEL OF PIEZOELECTRIC BEAMS

For the study of the stiffness of the layer was adopted the classic sandwich model (piezoceramic - bonding layer - host), as shown in figure 1. This allows the shear effect that will be responsible for one of the displacement losses of the layers. Thus, Bernoulli-Euler theory is retained for the outer layers, while the bonding layer (resin) is assumed to behave as a Timoshenko beam.

For the analysis of the output mechanical the resistance and inductance were optimization through on genetic algorithm in function of the a tension applied. Were is applied only in first mode of the vibration.

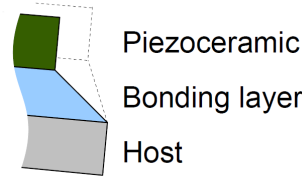


Figure 1: Schematic representation of reduction of transmissibility due to bonding layer.

With the applied theories of the Bernoulli and Timoshenko can be developed the equation of movement for the structure, this form the structure-patches-circuits coupled equations of motion can be written as

$$\begin{bmatrix} \mathbf{M} & \mathbf{0} \\ \mathbf{0} & \mathbf{L}_c \end{bmatrix} \begin{Bmatrix} \ddot{\mathbf{u}} \\ \ddot{\mathbf{q}}_p \end{Bmatrix} + \begin{bmatrix} \mathbf{C} & \mathbf{0} \\ \mathbf{0} & \mathbf{R}_c \end{bmatrix} \begin{Bmatrix} \dot{\mathbf{u}} \\ \dot{\mathbf{q}}_p \end{Bmatrix} + \begin{bmatrix} \mathbf{K}_m & -\bar{\mathbf{K}}_{me} \\ -\bar{\mathbf{K}}_{me}^t & \bar{\mathbf{K}}_e \end{bmatrix} \begin{Bmatrix} \mathbf{u} \\ \mathbf{q}_p \end{Bmatrix} = \begin{Bmatrix} \mathbf{F} \\ \mathbf{V}_c \end{Bmatrix}, \quad (1)$$

where \mathbf{u} and q_p are the global mechanical displacement and electric charge dofs and \mathbf{M} , \mathbf{K}_m , $\bar{\mathbf{K}}_{me}$, $\bar{\mathbf{K}}$ are the mass and mechanical, piezoelectric and dielectric stiffness matrices and \mathbf{F} is the mechanical force vector. \mathbf{L}_c and \mathbf{R}_c are diagonal matrices containing the inductance and resistance optimized and \mathbf{V}_c is the vector of electric voltage applied to the electric shunt circuits, but how in this work is studied only the output mechanical the value of the vector of electric voltage is equal zero.

3. VIBRATION CONTROL ANALYSIS

For vibration control analysis, the proposed model (Santos and Trindade 2011) is used to evaluate the mobility (velocity/force) frequency response function of the base structure. The resistive (R) or resonant (RL) shunt circuit affects both the passive and active-passive (hybrid) control performance. In this way, it became necessary to use the circuit that will dissipate the energy or to storage for later use.

3.1 Evaluation of mechanical output under mechanical excitation

How this work analyze a purely mechanical excitation, such as $V_c = 0$ and $F = bfe^{j\omega t}$, the amplitude of a displacement output $y = c_y \mathbf{u}$ can be written as $y = G_p(\omega) f$, where the FRF $G_p(\omega)$ is

$$G_p(\omega) = C_y \{ \omega^2 \mathbf{M} + J\omega \mathbf{C} + \mathbf{K}_m - \mathbf{K}_{me} (\omega^2 \mathbf{L}_c + J\omega \mathbf{R}_c + k_e)^{-1} \mathbf{K}_{me} \}^{-1} \quad (2)$$

Analyzing the equation 2 it can be noted that the resistance and the inductance have the capacity to change the rigidity properties of the piezoelectric material, in this way it will be applied to the case types i) open-circuit when R_c tending to infinity and ii) short-circuit when $L_c = R_c = 0$. For the open circuit it has

$$G_p^{oc}(\omega) = C_y \{ \omega^2 \mathbf{M} + J\omega \mathbf{C} + \mathbf{K}_m \}^{-1} \mathbf{b} \quad (3)$$

To the closed circuit

$$G_p^{sc}(\omega) = C_y \{ \omega^2 \mathbf{M} + J\omega \mathbf{C} + \mathbf{K}_m - \mathbf{K}_{me} \mathbf{K}_e \}^{-1} \mathbf{b} \quad (4)$$

You may note that no structural modification is observed in the open circuit box, whereas in the case of a short circuit, the rigidity of the piezoelectric patches is reduced.

3.2 Vibration control using piezoelectric actuators and state feedback

This way is necessary to rewrite the motion equations in the form of state space, containing the displacements and modal velocities of the piezoelectric patches and their derivatives of time.

$$\dot{\mathbf{z}} = \hat{\mathbf{A}}\mathbf{z} + \hat{\mathbf{B}}\mathbf{V}_c + \hat{\mathbf{B}}_f \mathbf{f}, \quad \mathbf{y} = \hat{\mathbf{C}}_y \mathbf{z}, \quad (5)$$

where

$$\mathbf{z} = \begin{bmatrix} \alpha \\ \mathbf{q}_p \\ \dot{\alpha} \\ \dot{\mathbf{q}}_p \end{bmatrix}, \quad \hat{\mathbf{A}} = \begin{bmatrix} \mathbf{0} & \mathbf{0} & \mathbf{I} & \mathbf{0} \\ \mathbf{0} & \mathbf{0} & \mathbf{0} & \mathbf{I} \\ -\Omega^2 & \mathbf{K}_p & -\mathcal{A} & \mathbf{0} \\ \mathbf{L}_c^{-1} \mathbf{K}_p^t & -\Omega_e^2 & \mathbf{0} & -\mathcal{A}_e \end{bmatrix}, \quad \hat{\mathbf{B}} = \begin{bmatrix} \mathbf{0} \\ \mathbf{0} \\ \mathbf{0} \\ \mathbf{L}_c^{-1} \end{bmatrix}, \quad \hat{\mathbf{B}}_f = \begin{bmatrix} \mathbf{0} \\ \mathbf{0} \\ \mathbf{b}_\phi \\ \mathbf{0} \end{bmatrix}, \quad \hat{\mathbf{C}}_y = [\mathbf{c}_\phi \quad \mathbf{0} \quad \mathbf{0} \quad \mathbf{0}]. \quad (6)$$

The modal displacements are such that $\mathbf{u} = \boldsymbol{\phi}\boldsymbol{\alpha}$ and, for mass normalized vibration modes, $\boldsymbol{\Omega}^2 = \boldsymbol{\phi}^t \mathbf{K}_m \boldsymbol{\phi}$ and $\boldsymbol{\Lambda} = \boldsymbol{\phi}^t \mathbf{C} \boldsymbol{\phi}$. $\boldsymbol{\Omega}$ is a diagonal matrix which elements are the undamped natural frequencies of the structure with piezoelectric patches in open-circuit. $\boldsymbol{\Omega}_e^2 = \mathbf{L}_c^{-1} \bar{\mathbf{K}}_e$ and $\boldsymbol{\Lambda}_e = \mathbf{L}_c^{-1} \mathbf{R}_c$ are both diagonal matrices which elements stand, respectively, for the squared natural frequencies of the electric circuits and the ratio between the resistances and inductances. The electromechanical coupling stiffness matrix projected in the undamped modal basis is defined as $\mathbf{K}_p = \boldsymbol{\phi}^t \bar{\mathbf{K}}_{me}$. Input \mathbf{b} and output \mathbf{c}_y distribution vectors are also defined, with modal projections $\mathbf{b}_\phi = \boldsymbol{\phi}^t \mathbf{b}$ and $\mathbf{c}_\phi = \mathbf{c}_y \boldsymbol{\phi}$, and \mathbf{f} is a vector of the amplitudes of each mechanical force applied to the structure (Santos and Trindade 2016).

A linear state feedback for the applied voltages \mathbf{V}_c is assumed such that $\mathbf{V}_c = -\mathbf{g}\mathbf{z} = -\mathbf{g}_{dm}\boldsymbol{\alpha} - \mathbf{g}_{de}\mathbf{q}_p - \mathbf{g}_{vm}\dot{\boldsymbol{\alpha}} - \mathbf{g}_{ve}\dot{\mathbf{q}}_p$, where \mathbf{g} is a matrix of control gains for each state variable. Therefore, the state space equation (5) becomes

$$\dot{\mathbf{z}} = (\hat{\mathbf{A}} - \hat{\mathbf{B}}\mathbf{g})\mathbf{z} + \hat{\mathbf{B}}_f \mathbf{f}, \quad \mathbf{y} = \hat{\mathbf{C}}_y \mathbf{z}. \quad (7)$$

For a single-input mechanical excitation f , the closed-loop or controlled amplitude of a single displacement output y can be written such that $\tilde{y} = G_h(\omega)\tilde{f}$, where the FRF $G_h(\omega)$ is

$$G_h(\omega) = \hat{\mathbf{C}}_y(j\omega\mathbf{I} - \hat{\mathbf{A}} + \hat{\mathbf{B}}\mathbf{g})^{-1} \hat{\mathbf{B}}_f, \quad (8)$$

which can also be derived from the second order equations of motion projected into the undamped modal basis leading to

$$G_h(\omega) = \mathbf{c}_\phi \left\{ -\omega^2 \mathbf{I} + j\omega(\boldsymbol{\Lambda} + \mathbf{K}_p \mathbf{D}_{cc}^{-1} \mathbf{g}_{vm}) + [\boldsymbol{\Omega}^2 + \mathbf{K}_p \mathbf{D}_{cc}^{-1} (\mathbf{g}_{dm} - \mathbf{K}_p^t)] \right\}^{-1} \mathbf{b}_\phi, \quad (9)$$

where the closed-loop dynamic stiffness of the electric circuit \mathbf{D}_{cc} is

$$\mathbf{D}_{cc} = -\omega^2 \mathbf{L}_c + j\omega(\mathbf{R}_c + \mathbf{g}_{ve}) + (\bar{\mathbf{K}}_e + \mathbf{g}_{de}). \quad (10)$$

The control gain \mathbf{g} can be calculated using the standard optimal LQR control theory applied to a single-input/single-output case, that is with only one active-passive patch-circuit pair for the control to minimize the vibration amplitude at one specific location of the structure, such that the following objective function is minimized

$$J = \frac{1}{2} \int_0^\infty (\dot{y}^2 + rV_c^2) dt, \quad (11)$$

where \dot{y} is the velocity at one location of interest and V_c is the control voltage applied to the active-passive shunt circuit in all cases following an iterative routine proposed in (Trindade, Benjeddou and Ohayon, 1999).

4. STOCHASTIC MODELING OF BONDING STIFFNESS FOR UNCERTAINTY QUANTIFICATION

Became an approach for analyzing random uncertainties for the bonding stiffness main parameter, that is the effective Young's modulus E of the adhesive. This is done considering the Young's modulus as a stochastic variable, respecting a given probability density function. Random realizations of the stochastic variable E are then generated. An appropriate probabilistic model for the stochastic variable is constructed accounting for the available information only, which is the following: (1) the support of the probability density function is $]0, +\infty[$; (2) the mean values are such that $E[X] = \underline{X}$; and (3) zero is a repulsive value for the positive-valued random variables which is accounted for by the condition $E[\ln(X)] = c_X$ with $|c_X| < +\infty$. Therefore, the Maximum Entropy Principle yields the following Gamma probability density functions for X (Soize, 2001; Cataldo et al., 2009; Ritto et al., 2010).

The probability density function for the adhesive Young's modulus is not known. Moreover, it is not possible to characterize its probability density function through of the measure physical, since the bonding stiffness depends not only on a manual mixture of two components (resin and hardener) but also on of the . Therefore, the effective bonding stiffness would have to be characterized after assembling.

Nevertheless, it is expected that a mean (or nominal) value could be estimated and, also, that it should be positive so a reasonable stochastic model can be constructed from a Gamma probability density function (pdf), present in equation 12.

$$p_E(E) = \mathbb{I}_{]0, +\infty[} \left(\frac{1}{\delta_E^2 \bar{E}} \right)^{\delta_E^{-2}} \frac{E^{\delta_E^{-2}-1}}{\Gamma(\delta_E^{-2})} \exp\left(-\frac{E}{\delta_E^2 \bar{E}}\right), \quad (12)$$

in which $\delta_E = \sigma_E/\bar{E}$ is the relative dispersion of stochastic bonding layer Young's modulus E_b and σ_E is its standard deviation. The Gamma function is defined as $\Gamma(x) = \int_0^\infty t^{x-1} e^{-t} dt$.

For comparative study, is necessary the use other density function distribution possessing mean of value upward of 2.5 Gpa. In this way probability density function considered for the adhesive Young's modulus is the Truncated Gaussian pdf. The Gaussian pdf, also known as Normal pdf, is given by

$$p_E(E) = \mathbb{I}_{]-\infty, +\infty[}(E) \frac{1}{\sigma_E \sqrt{2\pi}} e^{-\frac{(E-\bar{E})^2}{2\sigma_E^2}} \quad (13)$$

Notice that the support of the Gaussian pdf is $]-\infty, +\infty[$ and, thus, it may lead to negative values for the adhesive Young's modulus. Therefore, is be necessary to truncate the pdf in order to admit only positive values, considering $\bar{E} = 2.5$ GPa, $\delta_E = 94\%$, until all are within the range of acceptable. Figure 2a and Figure 2b shows the histograms of the samples generated with these parameters.

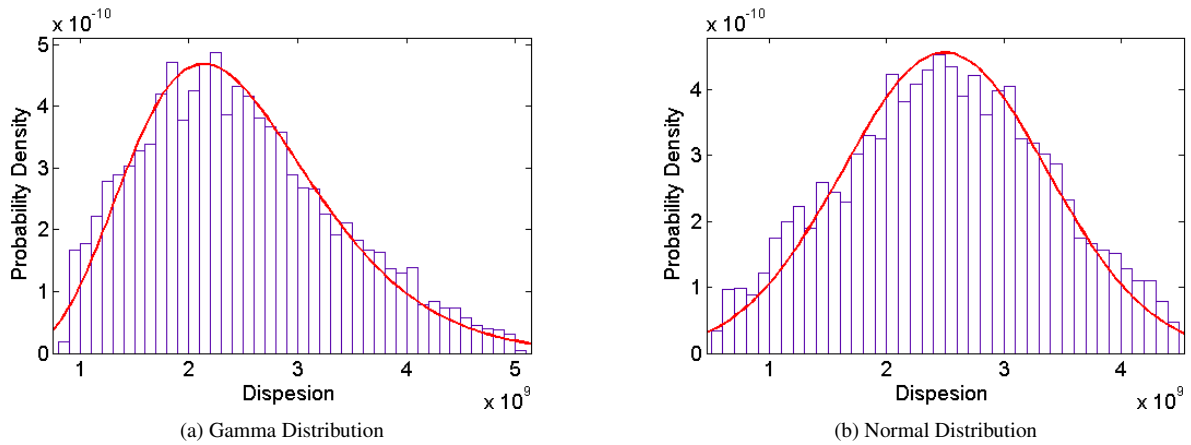


Figure 2: Histogram of samples using 5000 realizations

The histogram shown in Figure 2b follows very closely the expected behavior of a Gamma pdf with only positive values. However, it was observed that for this large value of relative dispersion, there is a concentration of realizations below 2 GPa.

The statistical analyses of the FRF amplitudes were performed using their 5000 realizations at each frequency to calculate the corresponding mean values and 95% confidence intervals. The 95% confidence intervals were evaluated using the 2.5% and 97.5% percentiles of the realizations of FRF amplitudes at each frequency. Figure ?? summarizes the simulation procedure.

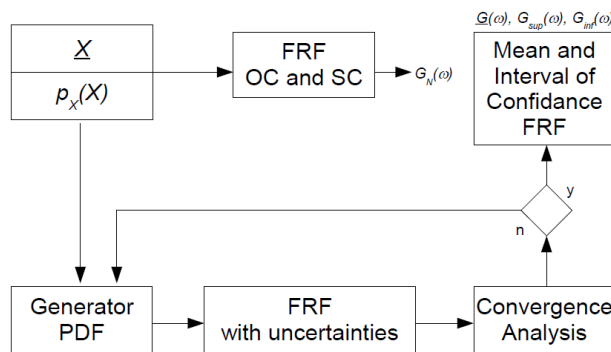


Figure 3: schematic representation of the computational procedure to obtain the confidence intervals for the frequency response functions $G_p(\omega)$ and $G_h(\omega)$

5. UNCERTAINTY QUANTIFICATION RESULTS

For analyzing random uncertainties Monte Carlo simulation were performed and the realizations of the frequency response functions, were used to evaluate their mean values and 95% confidence intervals, using 2.5% and 97.5% percentiles of the realizations. The effect of uncertainties about the efficiency were analyzed in function of the frequency response, where this case were applied only for the first mode of vibration. This where applied in the two distributions proposed.

5.1 Definition of the structure configuration

The structure is composed of a fixed beam of the aluminium of dimension 220 mm in length and width of 2 mm, the piezoelectric has a thick of 0.5 mm and is fixed by a layer of glue of 1 mm, as we can see in the figure 4. The extension piezoceramics are made of PZT-5H material whose properties are: $C_{D11} = 97.767$ GPa, $C_{D33} = 119.71$ GPa, $C_{D55} = 42.217$ GPa, $\rho = 7500$ kg m⁻³, piezoelectric coupling constants $h_{31} = 1.3520 \times 10^9$ N.C⁻¹ and $h_{15} = 1.1288 \times 10^9$ N.C⁻¹, and dielectric constants $\beta_{33} = 57.830 \times 10^6$ m.F⁻¹ and $\beta_{11} = 66.267 \times 10^6$ m.F⁻¹ (Santos and Trindade, 2011).

For the Aluminum beam using a two-part Epoxy bounding layer. Its material properties were considered to be deterministic: density 1160 kg m⁻³, nominal value of Young Modulus 2.5 GPa and Poisson ration equal to 0.3. The resistance and inductance were tuned to the first resonance frequency, using an optimization algorithm, leading to $Rc = 13.299$ K Ω and $Lc = 153.4063$ H. The purely passive action is obtained by eliminating the voltage source. For the general case, the inductance and resistance not only modify the dynamic stiffness of the structure, leading to damping and/or absorption, but also affects the harvesting effect. (Santos and Trindade, 2016).

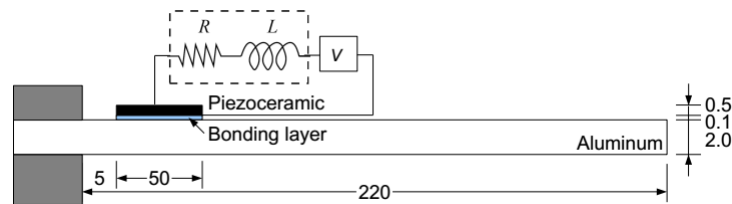


Figure 4: Representation of cantilever beam with bonded extension piezoceramic patch.

5.2 Gamma Probability Density Function

The Figure 5, can be observed the first mode from configuration presented in Figure 4 using the *p.d.f* Gamma developed in Figure 2a. For this configuration, the Figure 5 shows the mean and 95 % confidence interval for the frequency response of the shunted cantilever beam subjected to uncertainties of bonding layer stiffness compared to the short-circuit condition (without passive control). The interval of confidence presented an alteration on the resonance, making the peak of resonance displaced to the left, this represent more values lower 2.5 GPa in the Gamma probability density function. May notice that the nominal model indicates a passive reduction in the vibration amplitude of 21 dB (considering the difference between peak responses for SC and RL), while when considering the uncertainties is found to be in the range 15 dB for superior or 23 dB for inferior bound.

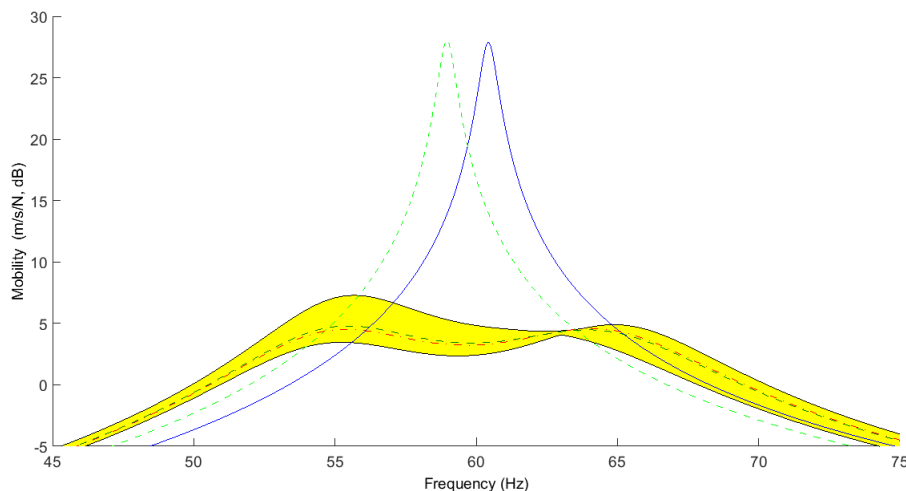


Figure 5: Mean (dashed) and nominal (solid) values and 95% confidence interval (filled) for the frequency response of the controlled cantilever beam, as compared to OC and SC conditions (dash-dot), subjected to uncertainties in E Passive shunt using Gamma Distribution *p.d.f*.

5.3 Normal Probability Density Function

The Figure 6, can be observed the first mode from configuration presented in Figure 4 using the *p.d.f* Normal developed in Figure 2b. For this configuration, the Figure 6 shows the mean and 95 % confidence interval for the frequency

response of the shunted cantilever beam subjected to uncertainties of bonding layer stiffness compared to the short-circuit condition (without passive control). The interval of confidence presented an alteration on the resonance, making the peak of resonance displaced to the left, this represent more values lower 2.5 GPa in the Normal probability density function. May notice that the nominal model indicates a passive reduction in the vibration amplitude of 23 dB (considering the difference between peak responses for SC and RL), while when considering the uncertainties is found to be in the range 18.5 dB for superior or 22 dB for inferior bound.

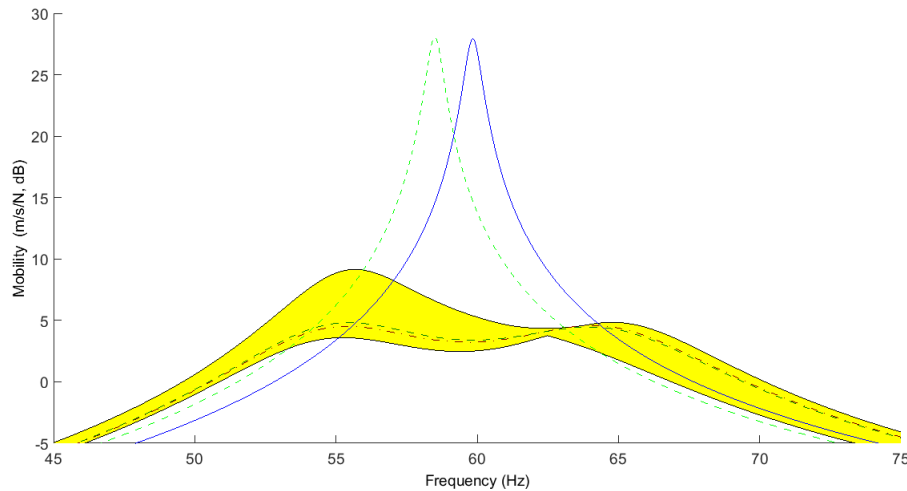


Figure 6: Mean (dashed) and nominal (solid) values and 95% confidence interval (filled) for the frequency response of the controlled cantilever beam, as compared to OC and SC conditions (dash-dot), subjected to uncertainties in E Passive shunt using Normal Distribution $p.d.f.$

6. CONCLUSION

An analysis of the effect of uncertainties of the bounding layer stiffness on the piezoelectric vibration control was performed. In passive (shunted) vibration control, bonding stiffness uncertainties mainly affect the tuning between electric circuit and piezo-structure, reducing the overall performance. Future works can be performed for new results using uncertainties on Poisson ratio and thickness of the layers.

7. REFERENCES

- S. Bhalla, P. Kumar, A. Gupta and T.K. Datta. Simplified impedance model for adhesively bonded piezo-impedance transducers. *Journal of Aerospace Engineering*, 22(4):373–382, 2009.
- A.R. de Faria and S.F.M. Almeida. Modeling of actively damped beams with piezoelectric actuators with finite stiffness bond. *Journal of Intelligent Material Systems and Structures*, 7(6):677–688, 1996.
- T.C. Godoy and M.A. Trindade. Modeling and analysis of laminate composite plates with embedded active-passive piezoelectric networks. *Journal of Sound and Vibration*, 330:194–216, 2011.
- T.C. Godoy and M.A. Trindade. Effect of parametric uncertainties on the performance of a piezoelectric energy harvesting device. *Journal of the Brazilian Society of Mechanical Sciences and Engineering*, 34(S12):552–560, 2012.
- N.W. Hagood and A. von Flotow. Damping of structural vibrations with piezoelectric materials and passive electrical networks. *Journal of Sound and Vibration*, 146(2):243–268, 1991.
- E.T. Jaynes. Information theory and statistical mechanics. *Physical Review*, 106(4):620–630, 1957.
- M. Pietrzakowski. Active damping of beams by piezoelectric system: effects of bonding layer properties. *International Journal of Solids and Structures*, 38:7885–7897, 2001.
- O. Rabinovitch and J.R. Vinson. Adhesive layer effects in surface-mounted piezoelectric actuators. *Journal of Intelligent Materials Systems and Structures*, 13:689–704, 2002.
- S.O. Reza Moheimani. A survey of recent innovations in vibration damping and control using shunted piezoelectric transducers. *IEEE Transactions on Control Systems Technology*, 11(4):482–494, 2003.
- T.G. Ritto, C. Soize and R. Sampaio. Stochastic dynamics of a drill-string with uncertain weight-on-hook. *Journal of the Brazilian Society of Mechanical Sciences and Engineering*, 32(3):250–258, 2010.
- H.F.L. Santos and M.A. Trindade. Structural vibration control using extension and shear active-passive piezoelectric networks including sensitivity to electrical uncertainties. *Journal of the Brazilian Society of Mechanical Sciences and Engineering*, 33(3):287–301, 2011.

- H.F.L. Santos and M.A. Trindade. Performance of active and passive vibration control using piezoelectric materials subjected to uncertainties on electrical and material properties. *Proceedings of the 1st International Symposium on Uncertainty Quantification and Stochastic Modeling*, Maresias, 2012.
- J. Sirohi and I. Chopra. Fundamental understanding of piezo-electric strain sensors. *Journal of Intelligent Materials Systems and Structures*, 11(4):246–257, 2000.
- C. Soize. Maximum entropy approach for modeling random uncertainties in transient elastodynamics. *Journal of the Acoustical Society of America*, 109(5):1979–1996, 2001.
- M. Sunar and S.S. Rao. Recent advances in sensing and control of flexible structures via piezoelectric materials technology. *Applied Mechanics Review*, 52(1):1–16, 1999.
- J. Tang, Y. Liu, and K.W. Wang. Semiactive and active-passive hybrid structural damping treatments via piezoelectric materials. *The Shock and Vibration Digest*, 32(3):189–200, 2000.
- O. Thomas, J. Ducarne, and J.-F. Deü. Performance of piezoelectric shunts for vibration reduction. *Smart Materials and Structures*, 21(1):015008, 2012.
- M.A. Trindade and A. Benjeddou. Hybrid active-passive damping treatments using viscoelastic and piezoelectric materials: review and assessment. *Journal of Vibration and Control*, 8(6):699–746, 2002.
- M.A. Trindade, A. Benjeddou and R. Ohayon. Parametric analysis of the vibration control of sandwich beams through shear-based piezoelectric actuation. *Journal of Intelligent Materials Systems and Structures*, 10(5):377–385, 1999.

8. RESPONSIBILITY NOTICE

The authors are the only responsible for the printed material included in this paper.